

Removal of Cr(III), Mn(II), Fe(III), Ni(II), Cu(II), Zn(II), and Pb(II) from Water Solutions Using Activated Carbon Based on Cherry Kernel Shell Powder

Khuder, Ali*⁺

Department of Chemistry, Atomic Energy Commission of Syria (AECS), P. O. Box 6091, Damascus, SYRIA

Koudsi, Yehya

Faculty of Chemistry, Damascus University, Damascus, SYRIA

Abboudi, Maher; Aljoumaa, Khaled

*Department of Radiation Technology, Atomic Energy Commission of Syria (AECS),
P. O. Box 6091 Damascus, SYRIA*

ABSTRACT: *In this work, a method for preparing activated carbon based on cherry kernel shell (AC-CKS) was investigated using two consecutive steps: chemical activation with H₂SO₄ agent and thermal activation in air. For the first time, AC-CKS product is used for the removal of numerous metal ions such Cr(III), Mn(II), Fe(III), Ni(II), Cu(II), Zn(II), and Pb(II) from water solutions. The AC-CKS was characterized using EA, FT-IR, SEM, EDX, and XRF techniques. The AC-CKS obtained by heating at 600 °C showed products with higher iodine numbers and invariably micro-size pores compared to those obtained by heating at 55°C and 400°C. The adsorption capacity of AC-CKS600 was tested in the removal of previously mentioned metal ions. The essential parameters affecting the removal of metal ions were studied. The results showed maximum adsorption of 99.0% for Cr(III), 91.7% for Fe(III), 62.0% for Cu(II), 59.3% for Pb(II), 42.0% for Zn(II), 28.0% for Ni(II), and 26.9% for Mn(II). The adsorption data of most metal ions fitted well with Langmuir model. The maximum adsorption capacity followed the sequence: Cr(10.75mg/g)>Fe(10.15mg/g)>Cu(7.58mg/g)>Pb(7.36mg/g)>Zn(6.08mg/g)>Ni(2.83g/g)>Mn(2.29 mg/g). The adsorption kinetics was tested for the pseudo-first order and pseudo-second order. The rate constants of adsorption for all studied metal ions were calculated. Good correlation coefficients ($R^2 > 0.9972$) were obtained for the pseudo-second-order kinetic model showing that all metal ions uptake processes followed the pseudo-second-order rate expression. Desorption studies showed the quantitative recovery of metal ions in the range of 89.4% for Pb(II) to 94% for Cr(III). According to the adsorption model applied in this work, AC-CKS600 product could be recommended for the removal of Cr(III), Fe(III), Cu(II), Pb(II), and Zn(II) from aqueous solutions.*

KEYWORDS: *Activated carbon; Adsorption; Cherry kernel shell; Metal ions.*

* To whom correspondence should be addressed.

+ E-mail: cscientific7@aec.org.sy

1021-9986/2022/11/3607-3625

19/\$/6.09

INTRODUCTION

Interest in the influence of heavy metals in the environment has been recently increased leading however to research intensification in the field of heavy metals removal from industrial and wastewaters. Numerous traditional methods have been used in this area, such chemical precipitation, coagulation, adsorption, ion exchange, electrolysis, and membrane filtration. Generally, these methods are costly and ineffective when the concentrations of heavy metals are limited [1,2]. In addition, most of the previous methods suffer from some drawbacks that limit its application such as high capital, operation costs and problem of disposal of residual metal sludge [3].

Alternative technologies for reducing metal concentrations in environment have been found by producing Activated Carbon (AC) on the basis of Agricultural Wastes (AWs), which are readily available and there are different production methods and target system applications for adsorbents [4-6]. The AWs, including rice husk, byproducts of soybeans, cottonseed hulls, rice straw, groundnut husk oxidized with silver, tea waste, watermelon shells, peanut hulls, were essentially used to adsorb Ni^{2+} , Pb^{2+} , Fe^{3+} , Zn^{2+} , Cr^{6+} , Cu^{2+} , Cd^{2+} , and As^{3+} from water solutions [7-13]. In addition, stones of many fruits including, date, olive, apricot, almond, peach, and cherry were considered as a major source of biomass in the food industry [14-18]. These stones were widely used in production of ACs [19-24] and adsorbents for the removal of heavy metal such Fe^{3+} , Co^{2+} , Ni^{2+} , Cu^{2+} , Zn^{2+} , Cd^{2+} , $\text{Cr}^{3+}/\text{Cr}^{6+}$, Pb^{2+} , Hg^{2+} from water solutions [2, 15, 20-23, 26-43]. Among the previously mentioned fruit stones, minor studies have been mentioned about cherry stones, although it is an inexpensive and abundant AW. However, Altun [25] used chitosan-coated sour cherry kernel shell beads for Cr^{6+} removal from acidic solutions; in further work, Altun and Ecevit [26] used F_2O_3 -chitosan-cherry kernel shell composite for the removal of Cr^{6+} from the aqueous solutions. *Pap et al.* [42] used a sulfur functionalized microporous biochar from an abundant biomass waste material (cherry kernels) for the selective removal of $\text{Pb}(\text{II})$ from landfill leachate. *Pap et al.* [43] reported an extended use of the AC based on the thermo-chemical conversion of the sweet and sour Cherry Kernel Shells (CKS). They used in their work ACs from CKS for separation of Pb^{2+} , Cd^{2+} , and Ni^{2+} from aqueous solutions.

AC-CKS product was prepared by physical activation method; the carbonization stage was usually carried out by heat treatment of a precursor at a given temperature in an inert atmosphere, whereas the activation stage was performed in air, carbon dioxide or steam atmosphere. In order to minimize the operational costs, as one of the main challenges of most research studies, AC could be synthesized in a complete absence of nitrogen as inert atmosphere [43]. The use of a chemical carbonization-based method with different reagents such H_2SO_4 , H_3PO_4 , and NaOH in aqueous solution was studied as an alternative to the physical carbonization method [19, 43, 44]. Many workers found that, the chemical activation was better than physical activation because of the lower temperatures and shorter activation time [45].

In connection with the previous findings, the present study was designed to prepare a new AC-CKS material, using optimal chemical activation conditions and followed by thermal activation at a relatively low temperature. In order to minimize the operational costs, the process of AC preparation was carried out in absence of atmosphere inert gases. Then, the prepared adsorbents were characterized through various instrumental analyses, comprising of Elemental Analysis (EA), FT-IR, SEM, EDX and BET, and their efficiency in removing some metal ions such as Cr^{3+} , Mn^{2+} , Fe^{3+} , Ni^{2+} , Cu^{2+} , Zn^{2+} , and Pb^{2+} from aqueous solutions were evaluated. After that, the effects of different process parameters such as pH of solution, adsorbent dosage, contact time and initial concentration on the separation efficiency of Cr^{3+} , Mn^{2+} , Fe^{3+} , Ni^{2+} , Cu^{2+} , Zn^{2+} , and Pb^{2+} from the aqueous solutions were investigated in the batch operational mode. Once the evaluation of the characteristics and the optimal process conditions was finalized, the equilibrium and kinetic of the adsorption in the batch operating system mode and their application ability in term of regeneration possibility were studied and evaluated.

EXPERIMENTAL SECTION

Sample collection and preparation

Cherry fruits were collected from Al-Zabadani city, which is located on the northwestern side of Damascus city, Syria. The flesh of cherry fruits was removed; then, the cherry stones were washed and the kernels were removed. After which, hard shells were dried at 60°C in an oven for 24 h, ground, and sieved with a 125- μ size sieve.

Shell powder was rested in 0.1 M HCl solution, extensively washed with distilled water to neutrality, and then dried at room temperature [25]. This kernel shell powder was called as Raw Cherry Kernel Shell (R-CKS).

Instrumentations and materials

The morphological study was investigated using a Scanning Electron Microscope (Tescan Vega II XMU, Czech) equipped with Energy Dispersive X-ray spectroscopy (SEM-EDX). The SEM magnifications were selected as 3000x. For these observations, the powder samples were placed on an adhesive conductive carbon disk. Chemical characterization was carried out by FT-IR spectroscopy in order to identify the functional groups at the surface of raw- and activated-carbon products. The IR spectra of the samples were recorded using a Nicolet 6700 FT-IR (Thermo, USA) operating in the range 4000–400 cm^{-1} and using KBr pellets with a resolution of 1 cm^{-1} . The pellet for infrared studies was prepared by mixing a given sample with KBr crystals and pressed into a pellet. In order to determine BET surface area, an automated gas adsorption analyzer, NOVA-2200e (Quantachrome Instruments, USA) was used with adsorption-desorption isotherms of nitrogen at -196°C .

The main contents of the elements, including C, H, and N were determined by EA method using an elemental analyzer, EURO EA 3000, EUROVECTOR, Milano, Italy. This analysis gave the mass percentages of carbon, hydrogen, and nitrogen in the samples simultaneously, and the mass percentage of oxygen was determined by subtraction. The accuracy of EA method was checked by the analysis of gas coal powder material (BCR no. 180 CRM) standard sample. To establish the reproducibility of the instrumental technique, three different standard samples weighted 0.001 g each were put in tin capsules and analyzed by the elemental analyzer.

Major and trace elements in raw and AC products were determined by X-Ray Fluorescence (XRF) technique (Oxford X-MET 5100 handheld elemental analyzer, Oxford, UK). The metal foils of Ti, V, Cr, Fe, Co, Ni, and Zn, with dimensions of 25x25 mm and 1 mm thickness each from Alfa Aesar, in addition to the pressed pellets of the single element of S (purity: 99%, Merck) and the stoichiometric compounds of KH_2PO_4 (purity: 99.5%, Merck), KCl (purity: 99.5%, Riedel-de Haen), CaCO_3 (purity: 99%, Riedel-de Haen), As_2O_3 (purity: 99.5%,

Merck), RbCl (purity: 99.0%, AppliChem), and SrCO_3 (purity: 98.0%, Fluka) were used for the XRF calibration of $\text{K}\alpha$ lines; while, the stoichiometric compounds of WO_3 (purity: 98%, LookChem), BaCl_2 (purity: 99%, Merck), Gd_2O_3 (purity: 99.9%, Fluka), $\text{Pb}(\text{NO}_3)_2$ (purity: 99%, Merck), and Nd_2O_3 (purity: 99.9%, Fluka) were used for the XRF calibration of $\text{L}\alpha$ lines. The pellets were pressed with a 2 cm diameter and around 1.0 g/cm^2 surface density each. The XRF spectra were evaluated using AXIL-QXAS software package that was developed by the International Atomic Energy Agency (IAEA) [46]. This program has the ability to determine the net peak area for each selected group of elements during the spectrum fitting. In the present work, the net peak areas of $\text{K}\alpha$ and $\text{L}\alpha$ lines of the elements in the standards were used in the calibration sensitivity of XRF technique. The sensitivities of the characteristic lines from the standards were then used to determine the concentrations of elements in the unknown samples of raw and AC materials using QXAS (quantitative X-ray analysis system) program [47]. The samples (0.05 g each) were put in polyethylene cups, having a sample area of ca. 0.1256 cm^2 . The polyethylene cups were covered from one side with Mylar foils. The accuracy of the XRF method was checked by the analysis of NIES CRM no. 9 Sargasso and fine fly ash (CTA-FFA-1) standard samples. To establish the reproducibility of the instrumental technique, five different standard subsamples with a mass of 0.05 g each were prepared and analyzed in a similar way as for the unknown samples.

The chemicals used in this work: H_2SO_4 , HNO_3 , HCl, NaOH, ammonia solution (NH_4OH), NaOH, sodium thiosulfate, and BaCl_2 salt were obtained from Merck; while, stock solutions of metals Cr, Mn, Fe, Ni, Cu, Zn, and Pb with 1000 mg/L were obtained from CHEM-LAB. All the chemical used were with the analytical grade.

Chemical activation

Preparation of AC was carried out according to the method of *Olivares-Marin et al.* [19] with some modifications, including the final concentration of H_2SO_4 solution, the temperature of the solution, and the contact time between R-CKS product and H_2SO_4 solution; taking into account the need to dilute the concentrated sulfuric acid solution, to prevent the filter paper from being destructed; while, heating of the solution was preferable to speed up the reaction between the raw material and

the acidic solution. Accordingly, mass of 20 g of R-CKS product was subjected for chemical activation in 200 mL of 98% concentrated sulfuric acid solutions. The obtained mixture was held in water bath at 40°C for 2 h. After which, the mixture was cooled at room temperature, diluted with distilled water to a volume of 500 mL, and allowed to stand for 24 h. Then, the obtained mixture was filtered through Whatman filter and washed frequently with distilled water until the filtrate was becoming free from sulfate ions. The presence of residual sulfate ions in the filtrate was identified by adding few drops of 0.412 mol/L BaCl₂ to the solution. Finally, the activated product was adjusted to pH 6.5-7 by 0.1 M NaOH solution, dried at 55°C until the successive weight differences were less than 5%, ground, sieved to particle size of 63 μm < r < 100 μm, and kept in desiccators for further work. The obtained product was called as AC-CKS55.

Thermal activation

To study the effect of thermal heating on the physicochemical characteristics and the adsorption capacity of the prepared activated carbons, two portions with 10 g each of AC-CKS55 were put in ceramic crucibles. Each portion was subjected to two steps of thermal activation. In the first step, the temperature was raised from ambient to 110°C at a rate of 15°C/min and held at this temperature for 30 min. In the second step, the first portion was subjected to temperature rise from 110°C to 400°C at a heating rate of 50°C/min. Then, it was held at the desired temperature for 30 min; while, the second portion was subjected to temperature rise from 110°C to 600°C at a heating rate of 82°C/min and held at the desired temperature for 30 min. After reaching the desired carbonization temperatures, the obtained AC products were allowed to cool down at room temperature, ground, sieved to particle sizes of 63 < r < 100 μm, and kept in an air tight polyethylene bags for further analyses. The products obtained by heating at 400°C and at 600°C were called as AC-CKS400 and AC-CKS600, respectively.

Characterization

The ACs were characterized as described elsewhere in terms of Iodine Number (IN), Bulk Density (BD), ash content (ASH), moisture content (MC), and BET surface area [19, 48, 49]. The IN was defined as the amount of iodine adsorbed by 1 g of carbon at the mg level.

The iodine adsorption was determined using the sodium thiosulfate volumetric method. The BD, ASH, and MC were determined by the methods reported by *Ekpete et al.* [49]. The apparent surface area was estimated using the Brunauer, Emmet and Teller (BET) equation in the relative pressure (P/P₀) range of 0.05–0.30. For each analysis, 0.2g of sample was used. The samples were degassed at 250°C for at least 12h.

Metal ion removal

The following seven metal ions: Cr³⁺, Mn²⁺, Fe³⁺, Ni²⁺, Cu²⁺, Zn²⁺, and Pb²⁺, which could be abundantly found in industrial and municipal wastewater [50,51], were chosen in this study. The effects of various parameters such as contact time, pH, adsorbent dosage, and initial metal ion concentrations on the removal of the metal ions by ACs were studied.

Adsorption experiments were made by a batch technique at room temperature and at different times. Known amounts (0.250 g) of prepared AC-CKS600 adsorbent were placed in different stoppered Erlenmeyer glass flasks, containing constant amounts (2.5 mg) of single metal ions. The pH solutions were adjusted to a constant value and the solutions were diluted with distilled water to a final volume of 25 mL. The solutions were shaken vigorously for a given time period to reach equilibrium. The agitation speed was kept constant (130 rpm) for each run to ensure equal mixing. After contact time 't' (min), the Erlenmeyer flasks containing the samples were withdrawn from the shaker. Then, the mixtures were filtered through filterpapers with 0.45 μm pore size, dried for 5 min at 55°C, and kept for further analysis by XRF technique. The removal percentage of metal ion from aqueous solutions (%) on AC-CKS600 adsorbent was calculated from Eq. (1):

$$\text{Removal (\%)} = \frac{C_t}{C_i} \times 100 \quad (1)$$

Where: C_t (mg/g) is the concentration of adsorbed metal ion on AC-CKS600 adsorbent at time 't', C_i (mg/g) is the metal ion concentration calculated from the Eq. (2):

$$C_i \text{ (mg/g)} = \frac{m_i}{m_{ads}} \quad (2)$$

Where: m_i (mg) is the total amount of metal ion added into the solution for adsorption on the adsorbent, and m_{ads} (g) is the amount of adsorbent.

To study the effect of pH, each single metal ion with initial concentration of 100 mg/L was adjusted to the desired pH value in the range 2-10. Then, 0.25 g of the AC-CKS600 adsorbent was added to each solution. After which, the obtained mixtures were agitated at room temperature of (25±1°C) using electrical shaker for a constant time (120 min) to attain equilibrium. The metal ions removed by AC-CKS600 product were filtered using filter papers with 0.45 µm pore size and dried for 5 min at 55°C. Finally, the removal concentrations of metal ions were determined by the XRF method.

The effect of adsorbent dosage was studied by varying the concentrations of AC-CKS600 from 2.0 g/L to 16.0 g/L, taking all other parameters constant: pH 8 for Cr(III) and pH 6 for the rest of metal ions, 25 mL final volume, 120 min contact time, and 100 mg/L initial metal ion concentration.

For the desorption studies, constant amounts (0.10 g) of the AC-CKS600, which were loaded separately with the studied metal ions (100 mg/L), were put in polyethylene bottles containing 10 mL of HNO₃ with concentrations in the range 0.025-0.15 M. The bottles were shaken at 130 rpm for 5 min. Then, the precipitates were filtered through filter paper with 0.45 µm, dried at 55°C for 5 min, and finally subjected to XRF analysis. To show the differences between the desorption efficiencies of acidic solutions; the previously mentioned procedure was also carried out by using HCl solutions.

Kinetic and isotherm studies

The removal amounts of metal ions at different agitation times (15 min–240 min) were determined. This experiment was conducted under the following conditions: initial metal ions concentrations of 10 mg/L; pH8 for Cr(III) and pH6 for the rest of metal ions; agitating speed 130 rpm; and 10 g/L of AC. The pseudo-first-order and pseudo-second-order were applied to predict the adsorption kinetics using the Eq. (3) and Eq. (4), respectively [52].

Pseudo-first-order-kinetic:

$$\ln(q_e - q_t) = -k_1t + \ln q_e \quad (3)$$

Where: q_e - the amount of metal ions adsorbed at equilibrium per unit weight of adsorbent (mg/g), q_t - the amount of metal ions adsorbed at any time (mg/g), k_1 - the adsorption rate constant.

Pseudo-second-order-kinetic:

$$\frac{t}{q_t} = \frac{1}{k_2q_e^2} + \frac{1}{q_e} t \quad (4)$$

Where: k_2 - the rate constant (g/mg/h).

The adsorption isotherm was also studied to determine the capacity of the ACs adsorbents. This was carried out by varying the initial metal ion concentrations (10 mg/L-200 mg/L), while the other parameters were remained constant as mentioned previously. The experimental adsorption equilibrium data were analyzed in terms of Langmuir and Freundlich isotherm models using Eq. (5) and Eq. (7), respectively [52].

Langmuir sorption isotherm:

$$\frac{1}{q_e} = \left(\frac{1}{b}\right) + \left(\frac{1}{ab}\right) \frac{1}{C_e} \quad (5)$$

Where: C_e - the metal ion concentration in the solution at equilibrium (mg/L), q_e - the metal ion concentration on the sorbent at equilibrium (mg/g), b and a are Langmuir constants, which are related to sorption capacity and energy of sorption, respectively.

The dimensionless constant separation factor is indicated by the following equation:

$$R_L = \frac{1}{(1 + aC_0)} \quad (6)$$

Where: 'a'- the Langmuir constant, C_0 - the initial concentration of metal ions. When $0 < R_L < 1$, the adsorption is favorable.

Freundlich sorption isotherm:

$$\log q_e = \log K_f + \frac{1}{N_f} \log C_e \quad (7)$$

Where: q_e and C_e - the equilibrium concentrations of metal ions in the adsorbent and liquid phases in mg/g and mg/L, respectively; K_f and N_f - are the Freundlich constants that are related to the sorption capacity and intensity.

RESULTS AND DISCUSSION

Composition of the adsorbents

The elements determined in the raw- and the prepared ACs samples were categorized into three groups: (i) the dominated elements (C, H, and N), (ii) the major elements, including K and Ca, and (iii) the trace elements, including Mn, Fe, Ni, Cu, Zn, Pb, Cr, and Ni. The suitability of EA technique for the determination of C, H, and N and XRF

Table 1: Analysis of standard samples by EA and XRF methods.

Sample	Element	Certified values	Obtained concentration	A ^a (%)	RSD ^b (%)
BCR no. 180 CRM (n=3)	C (mg/g)	760.1±2.1	758.4±2.7	-0.22	±0.36
	H (mg/g)	50.4±0.6	48.1±2.5	-4.56	±5.20
	N (mg/g)	14.4±0.3	13.7±0.9	-4.86	±6.57
NIES CRM no. 9 Sargasso (n=5)	K (mg/g)	61.0±2.0	59.1±3.3	-3.11	±5.58
	Ca (mg/g)	13.4±0.5	12.4±1.1	-7.46	±8.87
CTA-FFA-1 (n=5)	Fe (mg/g)	48.9±1.4	46.6±2.8	-4.66	±6.04
	Cr (µg/g)	156±8	163±16	+4.70	±9.82
	Cu (µg/g)	158.8±9	162±15	+1.89	±9.26
	Mn (µg/g)	1066±41	1045±97	-2.02	±9.28
	Ni (µg/g)	99.0±5.8	91.9±9.0	-7.17	±9.79
	Pb (µg/g)	369±46	373±28	+1.19	±7.45
	Zn (µg/g)	569±58	571±54	+0.35	±9.46

^a is the accuracy, which is estimated by the difference between the obtained and the certified values.

^b is the precision, which is estimated by a relative standard deviation.

technique for the determination of previously mentioned major and trace elements was checked by estimation of the accuracy and precision. The accuracy of EA method was estimated by the analysis of three subsamples of gas coal material (BCR no. 180 CRM); while the accuracy of XRF was estimated by the analysis of five subsamples of Sargasso (NIES CRM No. 9) and fly ash (CTA-FFA-1) standard samples each. The results in Table 1 showed that the elemental concentrations were in good agreement with the certified values with errors less than 5.0% for EA method and less than 7.5% for XRF method. The precision of the EA and XRF methods were evaluated in terms of the relative standard deviation, $RSD=(SD/C_i) \times 100$, where SD is the standard deviation and C_i is the mean of 'i' element concentrations. The results showed that the precision was better than ±6.6% and ±9.8% for the elements determined by EA and XRF methods, respectively.

The results showed that, the percentage concentrations values of C and O elements in the R-CKS product were of 52.0% and 39.5%, respectively, followed by H (6.16%) and N (0.80%). The concentrations of these elements were significantly affected by the thermal activation and were to a lesser extent by chemical activation. Thus, the concentration of C was extremely increased to 84.47% by chemical activation using H₂SO₄ agent and heating temperature at 600°C. In contrast, the concentrations of O

and H were gradually decreased by increasing the heating temperature. By the chemical treatment, the concentrations of major elements (K and Ca) in R-CKS were significantly decreased. In addition, concentrations of most studied trace elements were decreased by the chemical activations using H₂SO₄ agent and further heating at 600°C; the order of trace metal decreasing was as follows: Fe>Pb>Cu>Mn>Zn. On the other hand, Cr and Ni were obtained with concentrations below the XRF detection limits of 3.77 µg/g and 5.72 µg/g, respectively.

ACs characterization

The prepared ACs, i.e. AC-CKS55, AC-CKS400, and AC-CKS600, were characterized for yield, ASH, BD, MC, IN, and BET surface area (Table 2). The percentage yield of AC-CKS55 (69.4%) was higher than of AC-CKS400 (44.0%) and AC-CKS600 (38.4%). *Olivares-Marin et al.* [19], who denoted a smaller effectiveness of the chemical treatment to remove matter from ACs, also obtained a similar result. When H₂SO₄ solutions were used in the treatment of R-CKS, the product became blackish color and this denoted the occurrence of carbonization. Because H₂SO₄ represents an acid having oxidizing power and dehydration action, thus it could affect not only the organic fraction, but also its inorganic fraction. Chemical activation process followed by thermal heating at 600°C

Table 2: Physicochemical characteristics of ACs.

AC product	Characteristic					
	Yield (%)	ASH (%)	BD (g/mL)	MC (%)	IN (mg/g)	BET (m ² /g)
AC-CKS55	69.4	1.01	0.446	11.57	447	60
AC-CKS400	44.0	0.91	0.235	1.02	999	90
AC-CKS600	38.4	0.77	0.196	0.99	1194	183

showed higher effectiveness to produce ACs products with minimal ASH (0.77%) and BD (0.196 g/mL). The results showed that, drying the products of AC-CKS55, AC-CKS400, and AC-CKS600 involved the loss of the moisture present in the samples with a weight loss of 11.57 wt.%, 1.02 wt.%, and 0.99 wt.%, respectively. This indicated that ACs with higher thermal activations demonstrated a less hydrophilic character.

In the present work, the IN was used to estimate the surface area of the prepared activated carbons. IN was determined using the sodium thiosulfate volumetric method and estimated by the amount of iodine adsorbed by 1 g of AC at the mg level [48]. The results in Table 2 showed a surprisingly direct dependence of IN values on thermal activation temperatures. Thus, the higher activity level of the prepared ACs was achieved by applying the two following steps: (i) chemical activation of the raw material using concentrated H₂SO₄ solution; (ii) free water dehydration at a temperature of 110°C and subsequently thermal heating at 600°C. Accordingly, the iodine adsorbed by AC-CKS600 was 1194 mg/g, investigating AC based on cherry kernel shells with a large micro-pore structure, which could be due to the chemisorptions that took place in the pores of the carbons during carbonization and activation processes [53,54]. The BET surface areas of the obtained ACs at temperatures of 55°C, 400°C, and 600°C were 60 m²/g, 90 m²/g, and 183 m²/g, respectively, indicating the requirement to increase the temperature to obtain higher BET values. In this context, *Oliveras-Marin et al.* [19] prepared AC based on cherry stones using both of chemical and physical preparation methods; the BET surface area values of these ACs were lower than those obtained in the present work.

FT-IR and SEM analysis

Fig. 1 shows the FT-IR spectra of R-CKS, AC-CKS55, AC-CKS400, and AC-CKS600 samples. The absorption bands in the spectrum of R-CKS showed several functional

groups, including carboxyl, aromatic, alkene, hydroxyl, and carboxyl. This reflects the composition of CKS, which is mainly composed of cellulose, hemicelluloses and lignin [55]. The spectra of raw and activated carbons exhibited broad peaks attributing to O-H stretching group at 3435 cm⁻¹ and intensive peaks of conjugated ketone at 1635 cm⁻¹ [56].

R-CKS samples were affected by chemical and thermal activations. This was observed by absent or deformation of several peaks in the range from 2910 cm⁻¹ to 1058 cm⁻¹. Thus, the FT-IR spectrum of R-CKS had a peak that was observed at 2910 cm⁻¹ and attributed to the symmetric or asymmetric C-H stretching vibration of aliphatic acids; this peak was significantly decreased in AC-CKS55 material and totally absent from spectra of AC-CKS400 and AC-CKS600 materials. The peak observed at 1744 cm⁻¹ was due to the carboxyl stretching vibration of the carboxyl groups of pectin, hemicelluloses and lignin; this peak was absent in all of ACs products. The aromatic skeletal vibration in lignin was appeared at 1507 cm⁻¹, which was characteristic for lignin [57]; consequently, the absent of this peak indicated degradation of lignin during the chemical and thermal activation process of the prepared ACs. Peaks at 1459 cm⁻¹ and 1428 cm⁻¹ were observed for R-CKS material; these peaks could be due to C-H deformation in lignin, cellulose and hemicelluloses. The previous two peaks were overlapped after the chemical and thermal activations of the raw material. The band at 1377 cm⁻¹ could be due to C-H deformation in cellulose and hemicelluloses [58]; thermal heating of the AC product at 600°C intensively decreased this band. The peak at 1255 cm⁻¹ was related to aromatic C-N stretching [59]; this peak was absent in AC-CKS600 product. The absorption peak at 1050 cm⁻¹ was belonged to primary alcohol C-O stretch [56]; this peak was removed after thermal heating at 400°C and 600°C.

Fig. 2 shows the surface morphology of R-CKS, AC-CKS55, AC-CKS400, and AC-CKS600 products, which was studied using SEM with magnification of 3000x.

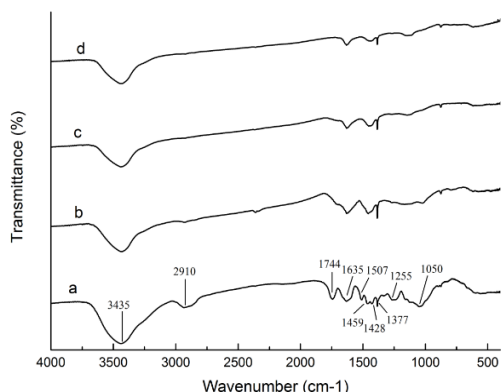


Fig. 1: FT-IR spectra of samples: *a* raw cherry kernel shell (R-CKS); *b* chemical treatment of R-CKS and drying at 55°C; *c* chemical treatment of R-CKS, followed by heating at 400°C, and *d* chemical treatment of R-CKS, followed by heating at 600°C.

In Fig. 2a, the R-CKS surface has consisted of particles with different dimensions ranging from 1x1.3 μm to 6x13.7 μm . R-CKS material exhibited rough surface morphology with little porosity. In contrast, the ACs samples (Fig. 2b-d) showed surface morphology with sponge-like structures. Relatively large holes with dimensions of 23.0x20.5 μm (19.6x16.0 – 27.0x25.3 μm) were clearly shown in Fig. 2b. Each hole contained several micro-size pores with different dimensions in the range (4.0x1.0 – 13.3x8.3 μm), indicating clear pores development during the chemical activation process. In Fig. 2c, the formation of well-developed pores at thermal activation of 400°C was obtained with a mean pore size of 23.4x20.4 μm (19.7x15.7 – 26.7x25.3 μm). By thermal heating at 600°C, Fig. 2d, the edges were pressed to form stretched pores with rough walls; the dimensions of these pores were in the range: 12.3x9.7 – 24.3x14.7 μm . *Anisuzzaman et al.* [60] also prepared ACs with sponge-like structures from *Typha orientalis* leaves using physical and chemical activation phosphoric acid (H_3PO_4), as dehydrating agent. These ACs were used for Pb(II) adsorption. The maximum adsorption capacity was found to be 7.95 mg/g.

Metal ions removal

Depending on the physicochemical results, the prepared AC-CKS600 product (prepared under conditions of chemical activation using H_2SO_4 agent and thermal heating at 600°C) was chosen for studying the removal efficiency of Cr(III), Mn(II), Fe(III), Ni(II), Cu(II), Zn(II),

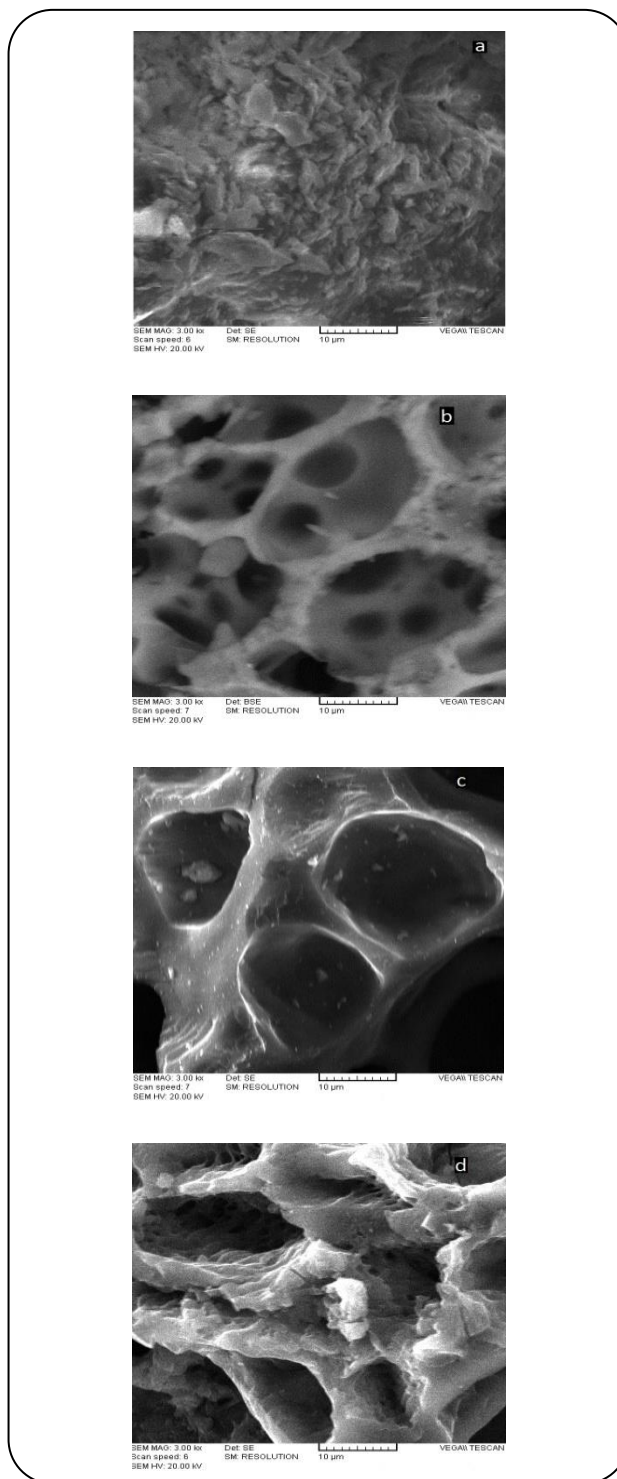


Fig. 2: SEM images of (a) raw cherry kernel shell; (b) chemically activated cherry kernel shell, followed by drying at 55°C; (c) chemically activated cherry kernel shell, followed by heating at 400°C; and (d) chemically activated cherry kernel shell, followed by heating at 600°C. Magnification at x3000.

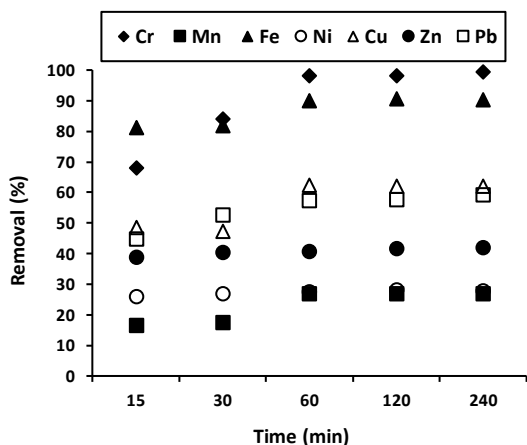


Fig. 3: Effect of contact time on the adsorption of heavy metals by AC-CKS600 adsorbent. Experimental conditions: Initial concentration of studied ions each was 100 mg/L, adsorbent dosage = 10 g/L for the removal of all metal ions, except Pb^{2+} ion which was removed using 16 g/L of the adsorbent, pH 8 for Cr(III) and pH 6 for the rest of metal ions, agitation speed = 130 rpm, and final volume of solution 25 mL.

and Pb(II) from aqueous solutions. For this purpose several parameters, such contact time, adsorbent dosage, pH, and initial concentration, were investigated.

The results in Fig. 3 showed that, the adsorption process of the metal ions reached the equilibrium state during a period ranging from 60 min to 240 min. At equilibrium, the adsorption process did not increase significantly due to the lack of vacant sites (pores) of adsorbents [29, 58]. Therefore the removal percentage means were roughly constants with values of: $99.5 \pm 2.3\%$ for Cr(III), $26.9 \pm 1.2\%$ for Mn(II), $90.3 \pm 2.9\%$ for Fe(III), $27.7 \pm 1.1\%$ for Ni(II), $62.1 \pm 2.0\%$ for Cu(II), $41.4 \pm 1.5\%$ for Zn(II), and $58.1 \pm 1.8\%$ for Pb(II), with relative standard deviation (RSD%) lower than 4.5 % for all studied metal ions. According to these results, the optimum contact time was selected as 120 min for further experimental studies. The optimum AC dosage chosen in this experiment was 10 g/L for the removal of all studied metal ions, except Pb^{2+} ion, which adsorbed using 16 g/L of the adsorbent.

The pH of the aqueous solution was considered as an important parameter for the adsorption of both anions and cations at the liquid–solid interface [61]. In fact, the pH dependency was related to both of the surface properties of the activated carbon and metal species in solution. In this work, the experiments were carried out at various initial

pH, ranging between 2 and 10 and at constant parameters: 25 mL final volume, 120 min contact time, and 10 g/L of AC for the removal of all studied metal ions, except Pb^{2+} which was adsorbed using 16 g/L of the adsorbent. The results obtained in this work (Fig. 4) were in good agreement with those reported by Abbas *et al.* [61]. These results included however the following types:

(i) First type was a strongly favorable adsorption equilibrium isotherm, including the adsorption of Cr(III), Fe(III), and Pb(II) ions. Thus, Cr(III) reached optimum adsorption value as high as 99% versus pH 8. Relatively, low percentages of Cr(III) were removed in acidic medium due to the presence of cationic form of hydroxides $Cr(OH)^{2+}$ and $Cr(OH)_2^+$ [62]. Accordingly, the removal of Cr(III) was 48.7% at pH 4, while this removal was increased to 86.5% at pH 6. It could be noted that, in acidic solutions, the carbon surface was positively charged and electrostatic interactions between Cr(III) species and activated carbon surface were unfavorable. In contrast, when the pH was increased to alkaline values, more sites that are negative were created and the removal of Cr(III) was improved. In a similar way, the adsorption of Fe(III) was increased up to pH 6, at which the optimum removal of Fe(III) was reached to 91.7%. The removal of Pb(II) ions was also increased by increasing the pH solution. The optimum removal of Pb(II) ions was obtained at pH 6 with a value of 59.3%; decreases in Pb(II) removal were obtained at $pH > 6$. This could be attributed to the presence of several lead species with different charges like $Pb(OH)^+$ and $Pb(OH)_2$ and thus the removal of lead was possibly accomplished by simultaneous precipitation of $Pb(OH)_2$ and sorption of $Pb(OH)^+$ [63].

(ii) Second type was a favorable adsorption equilibrium isotherm, including the adsorption of Cu(II) metal ions, which was efficiently increased in the pH range from 3 to 6. This could be due to the zero point of charge of the prepared adsorbent, which could lay between the previously mentioned pH ranges [64]. Thus, the optimum adsorption of Cu(II) was increased from 43.1% at pH 4 to 62.1% at pH 6.

(iii) Third type was a linear adsorption equilibrium isotherm, including the adsorption of Zn(II) ions at $pH \geq 4$.

(iv) Fourth type was an unfavorable adsorption equilibrium isotherm, including the adsorption of Mn(II) and Ni(II) ions. Slow increases in removal of Mn(II) and Ni(II) were obtained in the range of pH solution from 2 to 6.

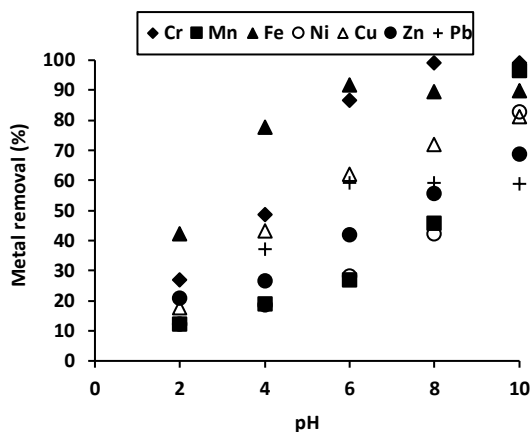


Fig. 4: Effect of pH on the adsorption of heavy metals by AC-CKS600 adsorbent. Experimental conditions: Initial concentration of studied ions each was 100 mg/L, adsorbent dosage = 10 g/L for the removal of all metal ions, except Pb^{2+} ions which was removed using 16 g/L of the adsorbent, agitation speed = 130 rpm, contact time 120 min, and final volume of solution 25 mL.

At pH 6, the optimum adsorptions of Mn(II) and Ni(II) were 26.9% and 28.0%, respectively. Extremely increases in removal of Mn(II) and Ni(II) ions were found at $pH \geq 8$. This could be attributed to the partial hydrolysis of Mn(II) and Ni(II) ions with increasing pH, bringing about the formation of complexes with OH⁻ [65, 66]. As a result, Mn and Ni hydroxyl species may participate in the adsorption and/or precipitation onto the adsorbent structure.

Depending on the previous experimental results, the adsorption mechanism analysis indicated that the adsorption of heavy metals was basically governed by the following essential parameters: (i) properties of ACs, (ii) experimental conditions, and (iii) properties of metal ions. Practically, changes in the surface of R-CKS were initiated after the chemical treatment. These changes were accompanied by presence of advanced holes in the surface of the adsorbent material; further improvement in the form and size of the holes was obtained by subjecting the ACs to thermal activation. Accordingly, the ACs were accompanied with quantitative decreases or an absence of some functional groups resulting by degradation of some fragments as lignin. In fact, the proposed process of AC preparation led to significant increases in BET surface area, which in turn revealed an increase in the adsorption capacity of the metal ions, but not to a large extent [67]. Olivares-Marín *et al.* [19] obtained similar results by

applying a similar process to prepare AC from cherry stones. The adsorption process could be explained as a result of three stages: film mass transfer, intra-particle diffusion, and chemical reaction on the adsorbent [68]. The initial rapid adsorption of metal ions on AC was due to rich adsorptive sites and large adsorption energy of activated carbon, the large external diffusion rate of the metal ions, and a small diameter of used metal ions [68]. In fact, this explanation was clearly agreed with the adsorption of Cr(III) and Fe(III), which have ions with triple valences and relatively small diameters.

It could be concluded that, the removal of the studied ions was preferably chosen at pH 8 for Cr(III) and pH 6 for the rest of metal ions in all subsequent experiments. According to these conditions, the removal percentages of the studied metal ions were decreased in the following order: Cr(III) > Fe(III) > Cu(II) > Pb(II) > Zn(II) > Ni(II) \approx Mn(II).

The concentration of metal ions removal was expected to be higher with higher initial concentrations, due to the transfer of metal ions from solution to surface of the AC. Fig. 5 shows the effect of initial metal ion concentration on the removal of the studied metal ions. The results confirmed the positive linear relationship between the removal of metal ions and the initial concentrations of all studied metal ions with correlation coefficients (R^2) better than 0.9773. This linearity was valid for the initial concentration range: 10-200 mg/L of all studied metal ions. The removal of metal ions was increased corresponding to the following ranges: Cr (0.870 – 14.4 mg/g), Mn (0.273 – 5.33 mg/g), Fe (0.920 – 13.1 mg/g), Ni (0.260 – 5.13 mg/g), Cu (0.720 – 13.9 mg/g), Zn (0.600 – 11.2 mg/g), and Pb (0.950 – 14.2 mg/g). These results indicated the potential application of AC-CKS600 product for the treatment of water containing metal ions of Cr(III), Mn(II), Fe(III), Ni(II), Cu(II), Zn(II), and Pb(II).

Adsorption kinetics

The pseudo-first-order kinetics and pseudo-second-order kinetics models (Fig. 6) were employed to study the kinetics of the studied metal ions. The adsorption rate constants (K_1 and K_2) and the adsorption capacity (q_e) were calculated from the adsorption slope and intercepts of the following functions: (i) $\log(q_e - q_t)$ versus 't' for the pseudo-first order and (ii) t/q_t versus 't' for the second-order. Rate constants K_1 and K_2 and the model prediction

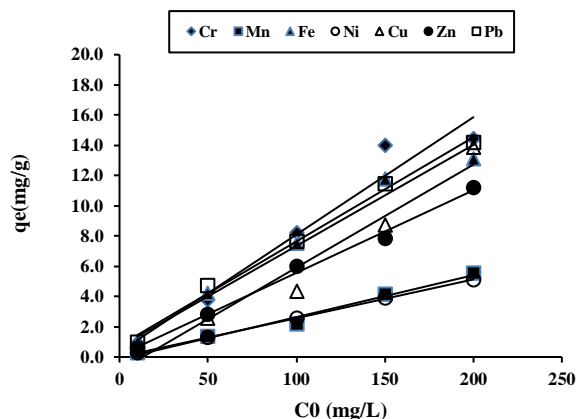


Fig. 5: The effect of initial metal ion concentration (C_0) on the removal of metal ions by AC-CKS600 adsorbent. Conditions: pH 8 for Cr(III) and pH 6 for the rest of metal ions; adsorbent dosage = 10 g/L for the removal of all metal ions, except Pb^{2+} ion which was removed using 16 g/L of the adsorbent; final volume 25 mL; contact time 120 min; agitation speed = 130 rpm.

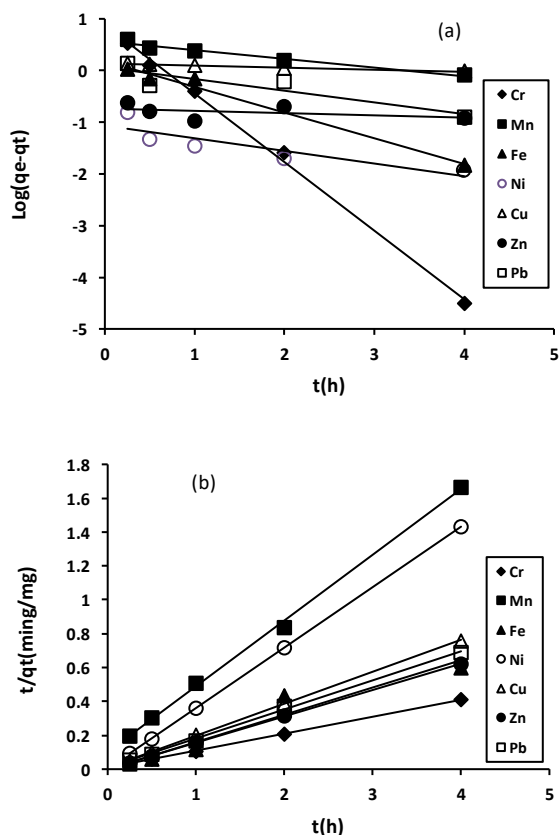


Fig. 6. Pseudo-first order (a) and pseudo-second order (b) plots at initial concentrations of 100 mg/L for all studied metal ions adsorption on ACHS-CKS600 adsorbent.

of q_e along with the experimental q_e values are shown in Table 3. According to these results, the pseudo-second-order adsorption model could reflect the adsorption mechanism, because it could fit well with heavy metal ion adsorption on the ACHS-CKS600 adsorbent. The values of R^2 based on pseudo second model were better than 0.99 for all used ion metals, and the $q_e(\text{theo})$ was fitted well with the corresponding $q_e(\text{exp})$. This suggested that the pseudo-second order model could describe the whole adsorption process of metal ions on AC-CKS600 and the chemical reaction played an important role during adsorption of all studied metal ions and was a rate-limiting step [68]. Overall, many studies showed the suitability of pseudo-second order model for describing the adsorption process of metal ions on ACs [69, 70].

The results showed that the values of $q_e(\text{theo})$, which were calculated from the pseudo-first-kinetic model, were clearly differed from the experimental values $q_e(\text{exp})$; while, for pseudo-second-order rate equation, $q_e(\text{theo})$ values were found to be in a very good agreement with those of $q_e(\text{exp})$ values. Furthermore, comparison of values of regression coefficient (R^2) factor confirmed that, the adsorption of all studied metal were followed the pseudo-second order kinetic model.

Adsorption isotherm

The adsorption of metal ions on AC-CKS600 product was tested using two isotherm equations, i.e. Langmuir and Freundlich. The isotherm constants were determined and given in Table 4.

The adsorption capacities based on Langmuir isotherm (Fig. 7) were with the following order for the studied metal ions:

$$\text{Cr(III)} > \text{Fe(III)} > \text{Cu(II)} > \text{Pb(II)} > \text{Zn(II)} > \text{Ni(II)} > \text{Mn(II)}$$

All R_L values were between 0 and 1 (Table 5), indicating the favorable adsorption for the studied metal ions on AC-CKS600 adsorbent. Based on the regression coefficient values, the Langmuir model was found to be more suitable for adsorption process of Cr(III), Mn(II), Fe(III), and Cu(II) metal ions, while both of Langmuir and Freundlich models were suitable for Ni(II), Zn(II) and Pb(II) metal ions (Table 4).

Comparison of maximum adsorption capacity values with those reported for other adsorbents are presented in Table 6 [20-23, 27, 28, 63, 65, 69, 71-80]. In the present work, a relatively good maximum adsorption of Cr(III) (10.75 mg/g) was obtained. This value was slightly lower

Table 3: Adsorption kinetics for ACHS-CKS600.

Metal ion	Concentration (mg/g)	qe(exp) (mg/g)	Pseudo-first-order			Pseudo-second-order		
			K1 (h ⁻¹)	R ²	qe(theo) (mg/g)	K2 (g/mg h)	R ²	qe(theo) (mg/g)
Cr	10	9.72	3.054	0.9966	7.58	0.9406	0.9995	10.36
Mn	10	2.40	0.387	0.9531	3.66	0.6740	0.9985	2.58
Fe	10	9.17	1.145	0.9852	1.52	1.9404	0.9998	9.27
Ni	10	2.80	0.563	0.7586	0.086	31.103	1.0000	2.80
Cu	10	6.21	0.092	0.9874	1.37	3.9606	0.9997	5.30
Zn	10	6.55	0.099	0.211	0.217	26.867	1.0000	6.43
Pb	10	5.94	0.521	0.8067	1.15	2.9120	0.9972	5.83

Table 4: Isotherm constants for AC-CKS600 adsorbent.

Metal ion	Langmuir model				Freundlich model		
	b (mg.g ⁻¹)	a (L.mg ⁻¹)	ab	R ²	K _f (mg.g ⁻¹)	N _f (L.mg ⁻¹)	R ²
Cr	10.75	0.603	6.49	0.9843	2.75	1.788	0.9722
Mn	2.29	0.007	0.016	0.9558	0.013	1.000	0.9372
Fe	10.15	0.111	1.12	0.9825	0.137	1.574	0.8766
Ni	2.83	0.013	0.037	0.9366	0.036	1.133	0.9323
Cu	7.58	3.91	29.65	0.9514	1.401	1.899	0.6545
Zn	6.08	33.68	204.63	0.9768	0.217	1.392	0.9768
Pb	7.36	9.00	66.29	0.9909	0.692	1.827	0.9995

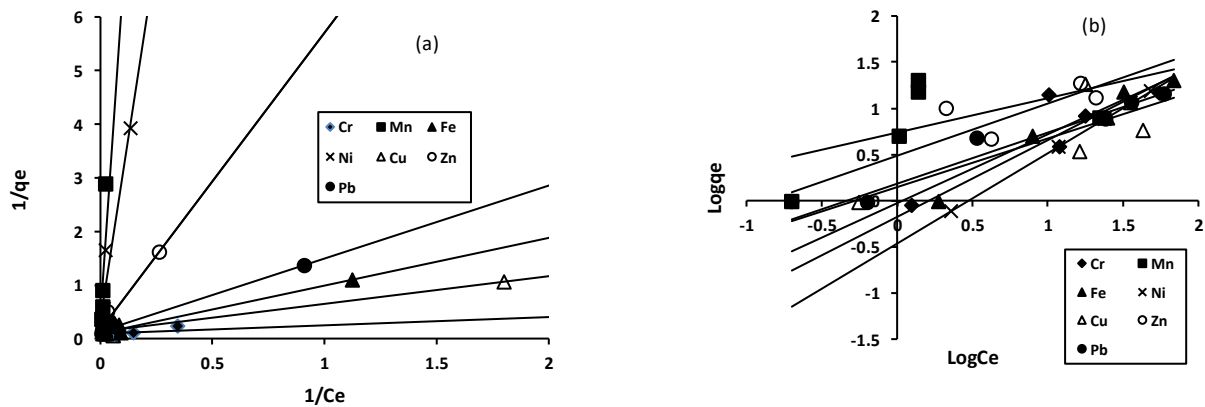


Fig.7. Langmuir(a) and Freundlich (b) isotherms for metal ion removal at various initial concentrations.

than those reported for activated carbon based on olive stone wastes [20] and moss [74], but better than that of Bulgarian lignite and bamboo activated carbon [64, 81]. The maximum adsorption capacity of Cr(III) was followed by that obtained for Fe(III), 10.15 mg/g. This value was better than that for Bulgarian lignite [64] and tannic acid

immobilized activated carbon [77]. In the present work, the maximum adsorption capacity of Cu(II) was 7.58 mg/g. This value was better than those reported for Bulgarian lignite and bamboo activated carbon [64, 80], but much lower than those for the other adsorbents such as apple tree branches, olive stone wastes, peanut shell, and

Table 5: R_L values based on the Langmuir isotherm for studied metal ions.

Co(mg/L)	Cr	Mn	Fe	Ni	Cu	Zn	Pb
10	0.1422	0.9333	0.4747	0.8855	0.0249	0.0030	0.0110
50	0.0321	0.7368	0.1531	0.6073	0.0051	0.0006	0.0022
100	0.0163	0.5832	0.0829	0.4360	0.0026	0.0003	0.0011
150	0.0109	0.4827	0.0568	0.3401	0.0017	0.0002	0.0007
200	0.0082	0.4117	0.0432	0.2788	0.0013	0.0001	0.0006

hazelnut [22, 27,72,76]. The maximum adsorption capacity of Zn(II) was 6.08 mg/g, indicating a comparable result reported for almond shells [28], but much lower than that reported for peanut shells [72]. Relatively low maximum adsorption capacities were obtained for Mn(II) and Ni(II) with values of 2.29 mg/g and 2.83 mg/g, respectively. These values were much lower than those values reported in the literature [21, 22, 65, 70, 72, 79], indicating poor adsorption capacity for Mn(II) and Ni(II). Finally, the maximum adsorption capacity obtained for Pb(II) was 7.36 mg/g. This value is better than that for maize cob and bamboo activated carbon [75, 80].

Desorption studies

The acidic solutions of HCl and HNO₃ were used for the desorption of metal ions that adsorbed on activated carbon materials [29, 81, 82]. However, by using 0.2 M HCl solution, Gebretsadik *et al.* [81] obtained a recovery rate of 80% of Cr(III) and Pb(II) that adsorbed on *Eucalyptus Camaldulensis*. In addition, Azam *et al.* [29] reported that the recovery of Cr(III) adsorbed on treated date seeds is better by using 0.1 M HCl than by using 0.1 M of NaOH, HNO₃, H₂SO₄, and CH₃COOH solutions. On the contrary, Kolodyńska *et al.* [82] found that 0.1 M HNO₃ solution is better than HCl and H₂SO₄ solutions for the recovery of ion metals such Cu(II), Zn(II), Cd(II), Co(II) and Pb(II) from biochar and activated carbon materials, while, higher concentrations could damage the structure of the AC sorbent. In the present work, desorption of metal ions was studied by using different concentrations (0.025-0.150 M) of nitric and hydrochloric acids. The results in Table 7 showed that, the recovery rate of Cr(III) was increased with increasing the concentration of HNO₃ or HCl solutions from 0.025 M to 0.100 M; with further increasing of HNO₃ and HCl concentrations, the recovery rate of Cr(III) remained roughly constant at 93.9% and 85.1% levels, respectively. In conclusion,

the results confirmed that, desorption mechanism was fast and the maximum recovery of Cr(III) was better by using 0.125 M HNO₃ solution. Desorption of other studied metal ions was obtained with the same manner as that for Cr(III).

CONCLUSIONS

Activated carbon based on locally available materials (cherry kernel shell) was successfully prepared by chemical activation process using H₂SO₄ agent, followed by thermal activation in air. The prepared AC in this work found to present several advantages such as its simplicity, low cost and low secondary environmental pollution.

Moreover, the characterization of activated carbon prepared by heating at 600°C (AC-CKS600) through different techniques revealed an adsorbent with exceptional properties such carbon abundance (84.5%), low inorganic matter level (0.77%), structure with well-developed porosity (micro-size pore), and maximum adsorption capacity (iodine number) of 1194 mg/g. Furthermore, this activated carbon had several reactive surface groups including carboxyl, hydroxyl, ketone and aromatic ones.

The AC-CKS600 adsorbent was applied for the first time with constant optimal conditions of pH, adsorbent mass, contact time, and agitation speed for removal of Cr(III), Mn(II), Fe(III), Ni(II), Cu(II), Zn(II), and Pb(II) from water solutions. Based on the regression coefficient values, the Langmuir model was found to be more suitable than the Freundlich for the metal ions of Cr(III), Mn(II), Fe(III), and Cu(II); while, the regression coefficient values showed that the adsorption process of Ni(II), Zn(II), and Pb(II) could be described by both Langmuir and Freundlich models. In accordance with the obtained results, the Langmuir adsorption capacity decreased in the following order: Cr(III)(10.75 mg/g) > Fe(III)(10.15) > Cu(II)(7.58 mg/g) > Pb(II)(7.36 mg/g) > Zn(II)(6.08 mg/g) > Ni(II)(2.83 mg/g) > Mn(II)(2.29 mg/g).

Table 6: Maximum adsorption capacities of metal ions onto activated carbons in this study and the other corresponding adsorbents in the literature.

Activated carbon precursor	Metal ion	pH	Metal ion adsorption capacity (mg/g)	References
Tannic acid immobilized activated carbon	Mn(II)	5.4	1.13	[77]
Graphene oxide/ZnO	Mn(II)	4.0	12.6	[70]
Granular Activated Carbon	Mn(II)	6.0	1.29	[79]
Modified- Granular Activated Carbon	Mn(II)	6.0	9.25	[79]
Cherry kernel shell	Mn(II)	6.0	2.29	Present work
Olive stone wastes	Cr(III)	9.0	14.3	[20]
Moss	Cr(III)	4.0	13.7	[74]
Bulgarian lignite	Cr(III)	4.5	2.07	[64]
Bamboo	Cr(III)	7.53	0.658	[80]
Cherry kernel shell	Cr(III)	8.0	10.75	Present work
Bulgarian lignite	Fe(III)	3.5	9.88	[64]
Tannic acid immobilized activated carbon	Fe(III)	4.2	1.77	[77]
Wood	Fe(III)	6.0	31.0	[78]
Cherry kernel shell	Fe(III)	6.0	10.15	Present work
Doum-palm seed coat	Ni(II)	7.0	13.51	[66]
Waste apricot	Ni(II)	5.0	101.01	[21]
Peanut shell	Ni(II)	4.8	26.35	[72]
Olive stone wastes	Ni(II)	5.7	14.65	[22]
Maize cob	Ni(II)	5.0	4.70	[75]
Commercial activated carbon	Ni(II)	5.0	3.18	[23]
Cherry kernel shell	Ni(II)	6.0	2.83	Present work
Bulgarian lignite	Cu(II)	4.5	4.09	[64]
Apple tree branches	Cu(II)	5.0	11.41	[76]
Olive stone wastes	Cu(II)	5.7	25.38	[22]
Peanut shell	Cu(II)	4.8	50.75	[72]
Hazelnut shell	Cu(II)	6.0	58.27	[27]
Bamboo	Cu(II)	8.16	1.908	[80]
Cherry kernel shell	Cu(II)	6.0	7.58	Present work
Almond shells	Zn(II)	5.0	6.65	[28]
Apple tree branches	Zn(II)	5.0	10.22	[76]
Olive stone wastes	Zn(II)	5.7	16.95	[22]
Peanut shell	Zn(II)	4.8	56.87	[72]
Cherry kernel shell	Zn(II)	6.0	6.08	Present work
Hazelnut shell	Pb(II)	5.7	13.05	[73]
Maize cob	Pb(II)	5.0	3.15	[75]
Peanut shell	Pb(II)	4.8	195.38	[72]
Bamboo	Pb(II)	7.83	1.998	[80]
Cherry kernel shell	Pb(II)	6.0	7.36	Present work

Table 7: Desorption rate of the system AC-CKS600/Cr(III) using different acids.

Acid concentration (M)	Desorption rate (%)	
	HNO ₃	HCl
0.025	65.8	38.8
0.050	82.7	50.9
0.075	90.3	65.0
0.100	92.3	85.6
0.125	93.9	85.1
0.150	93.9	85.0

Adsorption conditions: Initial concentration is 100 mg/L, adsorbent mass is 0.250 g, contact time is 30 min, final volume is 25 mL.

The kinetics of studied metal ions adsorption obeyed the pseudo-second-order model, suggesting however, chemisorption as the rate-limiting step in the adsorption process.

Acknowledgments

The author thanks Prof. I. Othman, Director General of AECS, for his encouragement and keen interest in this work. Thanks also due to head of Chemistry Department, Dr. A.W. Allaf, for his valuable advise.

Nomenclature

AC	Activated carbon
AC-CKS	Activated Carbon based on Cherry Kernel Shell
AC-CKS55	Treatment of Activated Carbon based on Cherry Kernel Shell at 55°C
AC-CKS400	Treatment of Activated Carbon based on Cherry Kernel Shell at 400°C
AC-CKS600	Treatment of Activated Carbon based on Cherry Kernel Shell at 600°C
ASH	Ash content
AWs	Agricultural Wastes
BET	Brunauer-Emmet-Teller
BD	Bulk Density
CKS	Cherry Kernel Shells
EA	Elemental Analysis
FT-IR	Fourier-Transfer Infrared spectroscopy
IN	Iodine Number
MC	Moisture Content
R-CKS	Raw- Cherry Kernel Shell

RSD	Relative Standard Difference
SEM	Scanning Electron Microscope
SEM-EDX	SEM with Energy-Dispersive X-ray spectroscopy
XRF	X-Ray Fluorescence

Received: Jun. 20, 2021 ; Accepted: Nov. 22, 2021

REFERENCES

- [1] Kapoor A., Viraraghavan T., [Fungal Biosorption - An Alternative Treatment Option for Heavy Metal Bearing Wastewaters: A Review](#), *Bioresour. Technol.*, **53(3)**: 195-206 (1995).
- [2] Blazquez G., Hernainz F., Calero M., Ruiz-Nunez L.F., [Removal of Cadmium Ions with Olive Stones: The Effect of Some Parameters](#), *Process Biochem.*, **40(8)**: 2649-2654 (2005).
- [3] Diniz V., Volesky B., [Desorption of Lanthanum, Europium and Ytterbium From Sargassum](#), *Sep. Purif. Technol.*, **50(1)**: 71-76 (2006).
- [4] Bhatnagar A., Hogland W., Marques M., Sillanpää M., [An overview of the Modification Methods of Activated Carbon for its Water Treatment Applications](#), *Chem. Eng. J.*, **219**: 499-511 (2013).
- [5] Ukanwa K.S., Patchigolla K., Sakrabani R., Anthony E., Mandavgane S., [A Review of Chemicals to Produce Activated Carbon from Agricultural Waste Biomass](#), *Sustainability*, **11(22)**: 6204 (2019).
- [6] Esmaeili A., Ghasemi S., Zamani F., [Investigation of Cr\(VI\) Adsorption by Dried Brown Algae Sargassum sp. and Its Activated Carbon](#), *Iran. J. Chem. Chem. Eng. (IJCCE)*, **31(4)**: 11-19 (2012).
- [7] Hegazi H.A., [Removal of Heavy Metals From Wastewater Using Agricultural and Industrial Wastes as Adsorbents](#), *J. Hous Built Environ.*, **9**: 276-282 (2013).
- [8] Hussain Sh., Abid M.A., Munawar Kh. Sh., Saddiqa A., Iqbal M., Suleman M., Hussain M., Riaz M., Ahmad T., Abbas A., Rehman M., Amjad M., [Choice of Suitable Economic Adsorbents for the Reduction of Heavy Metal Pollution Load](#), *Pol. J. Environ. Stud.*, **30(3)**: 1969-1979 (2021).
- [9] Dubey S.P., Gopal K., [Adsorption of Chromium\(VI\) on Low Cost Adsorbents Derived from Agricultural Waste Material: A Comparative Study](#), *J. Hazard. Mater.*, **145**: 465-470 (2007).

- [10] Wan Ngah W.S., Hanafiah M.A.K.M., [Removal of Heavy Metal Ions from Wastewater by Chemically Modified Plant Wastes as Adsorbents: A Review](#), *Bioresour. Technol.*, **99**: 3935-3948 (2008).
- [11] Mondal M.K., [Removal of Pb\(II\) Ions from Aqueous Solution Using Activated Tea Waste: Adsorption on a Fixed-Bed Column](#), *J. Environ. Manage.*, **90**: 3266-3271(2009).
- [12] Banerjee K., Ramesh S., Gandhimathi R., Nidheesh P., Bharathi K., [A Novel Agricultural Waste Adsorbent, Watermelon Shell for the Removal of Copper from Aqueous Solutions](#), *Iran. J. Energy Environ.*, **3(2)**: 143-156 (2012).
- [13] Massie B.J., Sanders T.H., Dean L.L., [Removal of Heavy Metal Contamination from Peanut Skin Extracts by Waste Biomass Adsorption](#), *J. Food Process. Eng.*, **38**: 555 (2015).
- [14] Ordoudi S.A., Bakirtzi Ch., Tsimidou M.Z., [The Potential of Tree Fruit Stone and Seed Wastes in Greece as Sources of Bioactive Ingredients](#), *Recycling*, **3(9)**: p.19 (2018).
- [15] Šoštarić T., Petrović M., Milojković J., Lačnjevac Č., Čosović A., Stanojević M., Stojanović M., [Application of Apricot Stone Waste from Fruit Processing Industry in Environmental Cleanup: Copper Biosorption Study](#), *Fruits*, **70**: 271-280 (2015).
- [16] Barral-Martinez M., Fraga-Corral M., Garcia-Perez P., Simal-Gandara J., Prieto M.A., [Almond By-Products: Valorization for Sustainability and Competitiveness of the Industry](#), *Foods*, **10(8)**: 1793 (2021).
- [17] Alharbi K.L., Raman J., Shin H.-J., [Date Fruit and Seed in Nutricosmetics](#), *Cosmetics*, **8(3)**: 59 (2021).
- [18] Bryś A., Bryś J., Obranović M., Škevin D., Głowacki S., Tulej W., Ostrowska-Ligęza E., Górska A., [Application of the Calorimetric Methods to the Characteristics of Seeds from Olives](#), *Proceedings*, **70(1)**: 90 (2021).
- [19] Olivares-Marín M., Fernández-González C., Macías-García Z.A., Gómez-Serrano V., [Preparation of Activated Carbon from Cherry Stones by Physical Activation in Air. Influence of the Chemical Carbonization with H₂SO₄](#), *J. Anal. Appl. Pyrol.*, **94**: 131–137 (2012).
- [20] Ba S., Ennaciri K., Yaacoubi A., Alagui A., Bacaoui A., [Activated Carbon from Olive Wastes as an Adsorbent for Chromium Ions Removal](#), *Iran. J. Chem. Chem. Eng. (IJCCE)*, **37**: 107-123 (2018).
- [21] Erdoğan S., Önal Y., Akmil-Başar C., Bilmez-Erdemoğlu S., Sarıci-Özdemir Ç., Köseoğlu E., İçduygu G., [Optimization of Nickel Adsorption from Aqueous Solution by Using Activated Carbon Prepared from Waste Apricot by Chemical Activation](#), *Appl. Surf. Sci.*, **252**: 1324–1331(2005).
- [22] Sharaf El-Deen G.E., [Sorption of Cu\(II\), Zn\(II\) and Ni\(II\) from Aqueous Solution Using Activated Carbon Prepared from Olive Stone Waste](#), *Adv. Environ. Technol.*, **3**: 147-161(2015).
- [23] Rahman M.M., Adil M., Yusof A.N.M., Ansary R.H., Yunus K., [Removal of Heavy Metal Ions with Acid Activated Carbons Derived from Oil Palm and Coconut Shells](#), *Materials*, **7(5)**: 3634-3650 (2014).
- [24] Aygun A., Yenisoy-Karakas S., Duman I., [Production of Granular Activated Carbon from Fruit Stones and Nutshells and Evaluation of their Physical, Chemical and Adsorption Properties](#), *Microporous Mesoporous Mater.*, **66**: 189–195(2003).
- [25] Altun T., [Chitosan-Coated Sour Cherry Kernel Shell Beads: An Adsorbent for Removal of Cr\(VI\) from Acidic Solutions](#), *J. Anal. Sci. Technol.*, **10**: 14 (2019).
- [26] Altun T., Ecevit H., [Cr\(VI\) Removal Using Fe₂O₃-Chitosan-Cherry Kernel Shell Pyrolytic Charcoal Composite Beads](#), *Environ. Eng. Res.*, **25(3)**: 426-438 (2020).
- [27] Demirbas E., Dizge N., Sulak M.T., Kobya M., [Adsorption Kinetics and Equilibrium of Copper from Aqueous Solutions Using Hazelnut Shell Activated Carbon](#), *Chem. Eng. J.*, **148**: 480–487 (2009).
- [28] Ferro-García M.A., Rivera-Utrilla J., Rodríguez-Gordillo J., Bautista-Toledo I., [Adsorption of Zinc, Cadmium, and Copper on Activated Carbons Obtained from Agricultural By-Products](#), *Carbon*, **26**: 363–373 (1988).
- [29] Azam M., Wabaidur S.M., Rizwan Khan M., Al-Resayes S.I., Islam M.S., [Removal of Chromium\(III\) and Cadmium\(II\) Heavy Metal Ions from Aqueous Solutions Using Treated Date Seeds: An Eco-Friendly Method](#), *Molecules*, **26**: 3718 (2021).
- [30] Khazaei I., Aliabadi M., Hamed Mosavian H.T., [Use of Agricultural Waste for Removal of Cr\(VI\) from Aqueous Solution](#), *Iran. J. Chem. Chem. Eng. (IJCCE)*, **8(4)**: 11-23 (2011).

- [31] Paredes-Doig A.L., Pinedo-Flores A., Aylas-Orejón J., Obregón-Valencia D., Sun Kou M.R., [The Interaction of Metallic Ions onto Activated Carbon Surface Using Computational Chemistry Software](#), *Adsorp. Sci. Technol.*, **0(0)**: 1–14 (2020).
- [32] Krishnamoorthy R., Govindan B., Banat F., Sagadevan V., Purushothaman M., Show P.L., [Date Pits Activated Carbon For Divalent Lead Ions Removal](#), *J. Biosci. Bioeng.*, **128(1)**: 88-97 (2019).
- [33] Banat F., Al-Asheh S., Al-Rousan D., [A Comparative Study of Copper and Zinc Ion Adsorption on to Activated and Non-activated Date-pits](#), *Adsorp. Sci. Technol.*, **20(4)**: 319-335(2002).
- [34] Corral-Bobadilla M., Lostado-Lorza R., Somovilla-Gómez F., Escribano-García R., [Effective Use of Activated Carbon from Olive Stone Waste in the Biosorption Removal of Fe\(III\) Ions from Aqueous Solutions](#), *J. Clean. Prod.*, **294(10)**: 126332 (2021).
- [35] Bohli Th., Quederni A., Fiol N., Villaescusa I., [Evaluation of an Activated Carbon from Olive Stones Used as an Adsorbent for Heavy Metal Removal from Aqueous Phases](#), *C.R.Chim.*, **18(1)**: 88-99 (2015).
- [36] Kobya M., Demirbas E., Senturk E., Ince M., [Adsorption of Heavy Metal Ions from Aqueous Solutions by Activated Carbon Prepared from Apricot Stone](#), *Bioresour. Technol.*, **96(13)**: 1518-1521 (2005).
- [37] Elamin A., Reddy M.R., Rehrah D., [Activated Carbon from Almond Shells to Adsorb the Heavy Metals from Contaminated Water](#), *Int. J. Chem. Environ. Technol.*, **1(3)**: (1-8) (2013).
- [38] Yahya M.D., Abubakar H., Obayomi K.S., Lyaka Y.A., Suleiman B., [Simultaneous and Continuous Biosorption of Cr and Cu \(II\) Ions from Industrial Tannery Effluent Using Almond Shell in a Fixed Bed Column](#), *Results Eng.*, **6**:100113 (2020).
- [39] Taha A.A., Moustafa A.H.E., Abdel-Rahman H.H., Abd El-Hameed N.M.A., [Comparative Biosorption Study of Hg\(II\) Using Raw and Chemically Activated Almond Shell](#), *Adsorp. Sci. Technol.*, **0(0)**: 1–28 (2017).
- [40] Rashed M.N., [Fruit Stones from Industrial Waste for the Removal of Lead Ions from Polluted Water](#), *Environ. Monit. Assess.*, **119**: 31–41 (2006).
- [41] Yan J., Lan G., Qiu H., Chen C., Liu Y., Du G., Zhang J., [Adsorption of Heavy Metals and Methylene Blue from Aqueous Solution with Citric Acid Modified Peach Stone](#), *Sep. Sci. Technol.*, **53(11)**: 1678-1688 (2018).
- [42] Pap S., Boyd K.G., Taggart M.A., Sekulic M.T., [Circular Economy Based Landfill Leachate Treatment with Sulphur-Doped Microporous Biochar](#), *Waste Manag.*, **124**: 160-171(2021).
- [43] Pap S., Radonić J., Trifunović S., Adamović D., Mihajlović I., Miloradov M.V., Sekulić M.T., [Evaluation of the Adsorption Potential of Eco-Friendly Activated Carbon Prepared from Cherry Kernels for the Removal of Pb²⁺, Cd²⁺ and Ni²⁺ from Aqueous Wastes](#), *J. Environ. Manage.*, **184**: 297-306 (2016).
- [44] Pietrzak R., Nowicki P., Kaźmierczak J., Kuszyńska I., Goscianskaa J., Przepiórski J., [Comparison of the Effects of Different Chemical Activation Methods on Properties of Carbonaceous Adsorbents Obtained from Cherry Stones](#), *Chem. Eng. Res. Des.*, **92(6)**: 1187-1191 (2014).
- [45] Hafizi-Atabak H. R., Ghanbari-Tuedeshki H., Shafaroudi A., Akbari M., Safaei-Ghomi J., Shariaty-Niassar M., [Production of Activated Carbon from Cellulose Wastes](#), *J. Chem. Pet. Eng.*, **47(1)**: 13-25 (2013).
- [46] IAEA [Quantitative X-ray Analysis System](#), User's Manual and Guide to X Ray Fluorescence Technique, Version 3.6, IAEA Laboratories Seibersdorf, International Atomic Energy Agency, Vienna, P. 161.
- [47] Khuder A., Bakir M., Solaiman A., Issa H., Habil Kh., Mohammad A., [Major, Minor, and Trace Elements in Whole Blood of Patients with Different Leukemia Patterns](#), *Nukleonika*, **57(3)**: 389–399 (2012).
- [48] Saka C., [BET, TG–DTG, FT-IR, SEM, Iodine Number Analysis and Preparation of Activated Carbon from A Corn Shell by Chemical Activation with ZnCl₂](#), *J. Anal. Appl. Pyrol.*, **95**: 21-24 (2012).
- [49] Ekpete O.A., Marcus A.C., Osi V., [Preparation and Characterization of Activated Carbon Obtained from Plantain \(*Musa paradisiaca*\) Fruit Stem](#), *J. Chem.*, **3**: 1-6 (2017).
- [50] Barakat M.A., [New Trends in Removing Heavy Metals from Industrial Wastewater](#), *Arab. J. Chem.*, **4(4)**: 361-377 (2011).
- [51] Marín-Rivera J.V., Martínez-Girón J., Quintero-Angel M., [Effectiveness of Vertical Subsurface Wetlands for Iron and Manganese Removal From Wastewater in Drinking Water Treatment Plants](#), *Univ. Sci.*, **24(1)**: 135-163 (2019).

- [52] Hema M., Srinivasan K., [Uptake of Toxic Metals from Wastewater by Activated Carbon from Agro Industrial by-Product](#), *Indian J. Eng. Mater. Sci.*, **17**: 373-381(2010).
- [53] Sugumaran P., Priya S.V., Rauichandran P., Seshadri S., [Production and Characterization of Activated Carbon from Banana Empty Fruit Bunch and Delonix Regia Fruit Pod](#), *J.Sustain Ener. Environ.*, **3**: 125–132 (2012).
- [54] Sahira J., Mandira A., Prasad B.P., Ram R.P., [Effect of Activating Agents on the Activated Carbons Prepared from Lapsi Seed Stone](#), *Res. J. Chem. Sci.*, **3(5)**: 19–24 (2013).
- [55] Roger M., Pettersen R.R., Tshabalala M.A., “Cell Wall Chemistry”, from: “Handbook of Wood Chemistry and Wood Composites”, CRC Press, London, UK, p. 34-70 (2012).
- [56] Nandiyanto A.B.D., Oktiani R., Ragadhita R., [How to Read and Interpret FTIR Spectroscopy of Organic Material](#), *Indones. J. Sci. & Technol.*, **4(1)**: 97-118 (2019).
- [57] Popescu C.M., Popescu M.C., Vasile C., [Structural Analysis of Photodegraded Lime Wood by Means of FT-IR and 2D IR Correlation Spectroscopy](#), *Int. J. Biol. Macromol.*, **48(4)**: 667–675 (2011).
- [58] Solihat N.N., Sari F.P., Risanto L., Anita S.H., Fitria F., Fatriasari W., Hermiati E., [Disruption of Oil Palm Empty Fruit Bunches by Microwave-assisted Oxalic Acid Pretreatment](#), *J. Math. Fund. Sci.*, **49(3)**: 244-257 (2017).
- [59] Kim M., Hwang S., Yu J.S., [Novel Ordered Nanoporous Graphitic C₃N₄ as a Support for Pt–Ru Anode Catalyst in Direct Methanol Fuel Cell](#), *J. Mater. Chem.*, **17(17)**: 1656-1659 (2007).
- [60] Anisuzzaman S.M., Joseph C.G., Daud W.M.A.B.W., Krishnaiah D., Yee H.S., [Preparation and Characterization of Activated Carbon from Typha Orientalis Leaves](#), *Int. J. Ind. Chem.*, **6**: 9–21 (2015).
- [61] Abbas S.H., Ismail I.M., Mostafa T.M., Sulaymon A.H., [Biosorption of Heavy Metals: A Review](#), *J. Chem. Sci. Technol.*, **3(4)**: 74-102 (2014).
- [62] Unceta N., Séby F., Malherbe J., Donard O.F.X., [Chromium Speciation in Solid Matrices and Regulation: A Review](#), *Anal. Bioanal. Chem.*, **397(3)**: 1097–1111 (2010).
- [63] Ramesh S.T., Rameshbabu N., Gandhimathi R., Kumar M.S., Nidheesh P.V., [Adsorptive Removal of Pb \(II\) from Aqueous Solution Using Nano-Sized Hydroxyapatite](#), *Appl. Water. Sci.*, **3(1)**: 105–113 (2013).
- [64] Vassileva P.St., Detcheva A.K., [Adsorption of Some Transition Metal Ions \[Cu\(II\), Fe\(III\), Cr\(III\) and Au\(III\)\] onto Lignite-based Activated Carbons Modified by Oxidation](#), *Adsorpt. Sci. Technol.*, **28(3)**: 229-242 (2010).
- [65] Omri A., Benzina M., [Removal of Manganese\(II\) Ions from Aqueous Solutions by Adsorption on Activated Carbon Derived A New Precursor: Ziziphus Spina-Christi Seeds](#), *Alex. Eng. J.*, **51(4)**: 343-350 (2012).
- [66] El-Sadaawy M., Abdelwahab O., [Adsorptive Removal of Nickel from Aqueous Solutions by Activated Carbons from Doum Seed \(Hyphaenethebaica\) Coat](#), *Alex. Eng. J.*, **53(2)**: 399-408 (2014).
- [67] Kuroki A., Hiroto M., Urushihara Y., Horikawa T., Sotowa K.I., Avila J.R.A., [Adsorption Mechanism Of Metal Ions On Activated Carbon](#), *Adsorption*, **25**: 1251–1258 (2019).
- [68] Tang C., Shu Y., Zhang R., Li X., Song J., Li B., Zhang Y., Ou D., [Comparison of the Removal and Adsorption Mechanisms of Cadmium and Lead from Aqueous Solution by Activated Carbons Prepared from Typha Angustifolia And Salix Matsudana](#), *RSC Adv.*, **7**: 16092-16103 (2017).
- [69] Doulia D., Leodopoulos Ch., Gimouhopoulos K., Rigas F., [Adsorption of Humic Acid on Acid-Activated Greek Bentonite](#), *J. Colloid Interface Sci.*, **340(2)**: 131–141 (2009).
- [70] Leiva E., Tapia C., Rodríguez C., [Removal of Mn\(II\) from Acidic Wastewaters Using Graphene Oxide–ZnO Nanocomposites](#), *Molecules*, **26**, 2713, p.18 (2021).
- [71] Moussa S.I., Ali M.M.S., R.R. Sheha, [The Performance of Activated Carbon/NiFe₂O₄ Magnetic Composite to Retain Heavy Metal Ions From Aqueous Solution](#), *Chin. J. Chem. Eng.*, **29**: 135-145 (2021).
- [72] Wilson K., Yang H., Seo C.W., Marshall W.E., [Select Metal Adsorption by Activated Carbon Made From Peanut Shells](#), *Bioresour. Technol.*, **97**: 2266–2270 (2006).

- [73] Imamoglu M., Tekir O., [Removal of Copper \(II\) and Lead \(II\) Ions from Aqueous Solutions by Adsorption on Activated Carbon from a New Precursor Hazelnut Husks](#), *Desalination*, **228**: 108–113 (2008).
- [74] Low K.S., Lee C.K., Tan S.G., [Sorption of Trivalent Chromium from Tannery Waste by Moss](#), *Environ. Technol.*, **18**(4): 449–454 (1997).
- [75] Nale B. Y., Kagbu J. A., Uzairu A., Nwankwere E. T., Saidu S., Musa H., [Kinetic and Equilibrium Studies of the Adsorption of Lead\(II\) and Nickel\(II\) Ions from Aqueous Solutions on Activated Carbon Prepared from Maize Cob](#), *Der Chemica Sinica*, **3**(2): 302-312 (2012).
- [76] Zhao S., Ta N., Wang X., [Absorption of Cu\(II\) and Zn\(II\) from Aqueous Solutions onto Biochars Derived from Apple Tree Branches](#), *Energies*, **13**, 3498, p.19. (2020).
- [77] Üçer A., Uyanik A., Aygün Ş.F., [Adsorption of Cu\(II\), Cd\(II\), Zn\(II\), Mn\(II\) and Fe\(III\) Ions by Tannic Acid Immobilised Activated Carbon](#), *Sep. Purif. Technol.*, **47**(3): 113-118 (2006).
- [78] Kouakou U., Ello A.S., Yapo J.A., Trokourey A., [Adsorption of Iron and Zinc On Commercial Activated Carbon](#), *J. Environ. Chem. Ecotoxicol.*, **5**(6): 168-171 (2013).
- [79] Tran T.N., Kim D.G., Ko S.O., [Adsorption Mechanisms of Manganese \(II\) Ions onto Acid-treated Activated Carbon.](#), *KSCE J. Civ. Eng.*, **22**: 3772–3782 (2018).
- [80] Lo S.F., Wang S.Y., Tsai M.J., Lin L.D., [Adsorption Capacity and Removal Efficiency of Heavy Metal Ions by Moso and Ma Bamboo Activated Carbons](#), *Chem. Eng. Res. Des.*, **90**: 1397–1406 (2012).
- [81] Gebretsadik H., Gebrekidan A., Demlie L., [Removal of Heavy Metals from Aqueous Solutions Using Eucalyptus Camaldulensis: An Alternate Low Cost Adsorbent](#), *Cogent Chem.*, **6**: 1720892 (2020).
- [82] Kołodyńska D., Krukowska J., Thomas P., [Comparison of Sorption and Desorption Studies of Heavy Metal Ions From Biochar and Commercial Active Carbon](#), *Chem. Eng. J.*, **307**: 353-363 (2017).